

Cathode-Supported All-Solid-State Lithium-Sulfur Batteries with High Cell-Level Energy Density

Ruochen Xu, Jie Yue, Sufu Liu, Jiangping Tu, Fudong Han, Ping Liu, and Chunsheng Wang

ACS Energy Lett., **Just Accepted Manuscript** • DOI: 10.1021/acsenerylett.9b00430 • Publication Date (Web): 12 Apr 2019

Downloaded from <http://pubs.acs.org> on April 17, 2019

Just Accepted

"Just Accepted" manuscripts have been peer-reviewed and accepted for publication. They are posted online prior to technical editing, formatting for publication and author proofing. The American Chemical Society provides "Just Accepted" as a service to the research community to expedite the dissemination of scientific material as soon as possible after acceptance. "Just Accepted" manuscripts appear in full in PDF format accompanied by an HTML abstract. "Just Accepted" manuscripts have been fully peer reviewed, but should not be considered the official version of record. They are citable by the Digital Object Identifier (DOI®). "Just Accepted" is an optional service offered to authors. Therefore, the "Just Accepted" Web site may not include all articles that will be published in the journal. After a manuscript is technically edited and formatted, it will be removed from the "Just Accepted" Web site and published as an ASAP article. Note that technical editing may introduce minor changes to the manuscript text and/or graphics which could affect content, and all legal disclaimers and ethical guidelines that apply to the journal pertain. ACS cannot be held responsible for errors or consequences arising from the use of information contained in these "Just Accepted" manuscripts.



Cathode-Supported All-Solid-State Lithium-Sulfur Batteries with High Cell-Level Energy Density

Ruochen Xu^{†,‡} Jie Yue[†] Sufu Liu^{†,‡} Jiangping Tu[‡] Fudong Han^{,†} Ping Liu^{*,§} and Chunsheng Wang^{*,†}*

[†]Department of Chemical and Biomolecular Engineering, University of Maryland, College Park, Maryland 20742, United States

[‡]State Key Laboratory of Silicon Materials, Key Laboratory of Advanced Materials and Applications for Batteries of Zhejiang Province, and School of Materials Science& Engineering, Zhejiang University, Hangzhou 310027, China

[§]Department of Nanoengineering, University of California, San Diego, La Jolla, California 92093, United States

AUTHOR INFORMATION

Corresponding Author

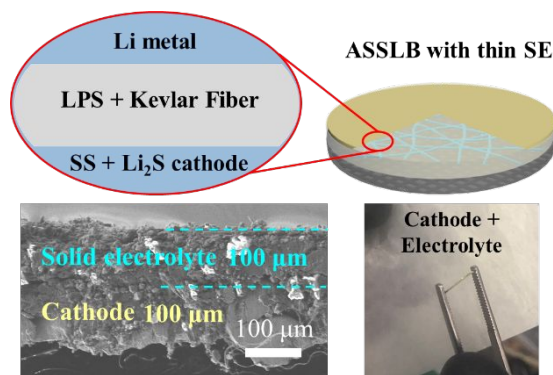
*Email: fdhan@umd.edu

*Email: piliu@eng.ucsd.edu

*Email: cswang@umd.edu

ABSTRACT. Bulk-type all-solid-state lithium batteries (ASSLBs) are being considered as a promising technology to improve the safety and energy density of today's batteries. However, current bulk-type ASSLBs suffer from low cell-level energy density due to the challenges in reducing the electrolyte thickness. In this work, we report a cathode-supported ASSLBs with a thin solid electrolyte layer. Starting from a stainless-steel mesh supported Li_2S cathode, we are able to build an ASSLB with a $\sim 100\ \mu\text{m}$ thick Li_3PS_4 electrolyte reinforced by Kevlar nonwoven scaffold and with Li metal as the anode. The ASSLB delivers a high capacity with high rate and cycling performances at room temperature. Moreover, the unique cell design also enabled to utilize a thick cathode with a Li_2S loading of $7.64\ \text{mg cm}^{-2}$, providing a high cell-level energy density (excluding the current collectors) of $370.6\ \text{Wh Kg}^{-1}$ for the first cycle.

TOC GRAPHICS



All-solid-state lithium batteries (ASSLBs) hold great potential to significantly improve the safety and energy density of today's lithium ion batteries by using nonflammable, inorganic solid

electrolytes.¹⁻³ Solid electrolytes play a critical role in enabling ASSLBs. Among various lithium ion conducting materials, sulfide-based solid electrolytes are one of the most promising electrolytes because of their excellent ionic conductivity and mechanical property.⁴⁻⁵ The ionic conductivities of several sulfide electrolytes are comparable with or even higher than that of the organic liquid electrolyte,⁴⁻⁹ enabling all-solid-state lithium ion batteries with very high cycling and rate performances.^{5, 10-13} However, a very thick solid electrolyte ($\sim 0.5\text{--}1.0$ mm) was usually used in these ASSLBs.^{5, 14-18} As a result, the cell-level energy densities of these ASSLBs are still limited to < 200 Wh kg^{-1} which is lower than that of the commercialized lithium ion batteries.

There are many reports about preparing thin electrolyte layers¹⁹⁻²⁴. For example, Lee prepared a $64\text{ }\mu\text{m}$ -thick electrolyte by creating a solid electrolyte-in-polymer matrix.¹⁹ Jung reported the fabrication of a $70\text{ }\mu\text{m}$ -thick sulfide electrolyte using poly(paraphenylene terephthalamide) nonwoven scaffold as a mechanical support.²⁰ In addition, a sub-micrometer-solid electrolyte membrane was also prepared using a self-assembly approach.²¹ However, integrating these thin electrolytes into a high-energy cell (e.g. Li/S) has never been achieved because the thin electrolyte layer is easy to break during cell fabrication or operation, especially for the S cathode and Li anode with a large volume change. Therefore, the cathode materials used in these cells are LiCoO_2 and FeS_2 , while the anode materials are graphite, $\text{Li}_4\text{Ti}_5\text{O}_{12}$, and Li-In alloy,¹⁹⁻²⁰ limiting the energy densities of ASSLBs.

In this present study, we report a method for fabricating a cathode-supported ASSLBs with a thin electrolyte. Different from the conventional electrolyte-supported cell that starts from the fabrication of the electrolyte layer and then the assembly of electrodes layers on each side of the electrolyte, we start to build the cell from a stainless-steel supported Li_2S cathode. Using a Kevlar nonwoven scaffold as mechanical support, a $\sim 100\text{ }\mu\text{m}$ -thick Li_3PS_4 (LPS) glass solid electrolyte was successfully integrated in the Li/S ASSLBs. The all-solid-state Li/S batteries with a Li_2S loading of 2.54 mg cm^{-2} provided a high initial capacity of 949.9 mAh g^{-1} at 0.05 C at room temperature. Moreover, the cell also exhibited great performance when increasing the loading of Li_2S to 7.64 mg cm^{-2} and a high energy density of 370.6 Wh kg^{-1} in a cell level (excluding current collectors) was achieved. Our work provides a new approach for fabricating ASSLIBs with high energy densities.

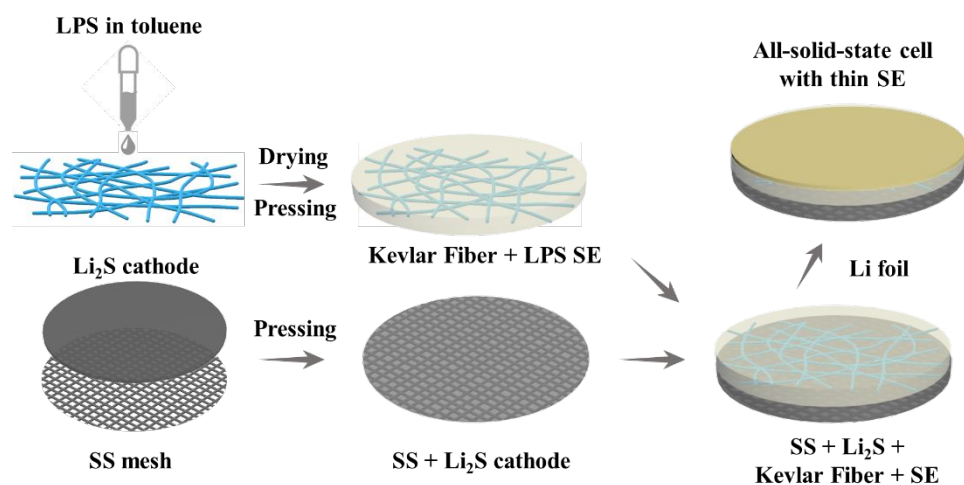


Figure 1. Schematic illustration of the fabrication of the cathode-supported all-solid-state cell with a thin sulfide electrolyte.

Figure 1 shows the schematic illustration of the fabrication process of all-solid-state cell with thin sulfide electrolytes. Li_2S - LiI solid solution is used as the active material for the cathode because adding LiI into Li_2S can effectively improve the ionic conductivity of Li_2S ,²⁵ which helps to improve the kinetics of the cathode. The ionic conductivity of the as-prepared Li_2S - LiI is measured to be $2.6 \times 10^{-6} \text{ S cm}^{-1}$ (Figure S1), which is about two orders of magnitude higher than that of Li_2S .²⁶ The active material is mixed with vapor grown carbon fiber (VGCF) and LPS glass electrolyte with a weight ratio of 75:10:15 to make the cathode. Detailed characterizations of the cathode composite can be found in the Supporting Information (Figures S2-S4). The main peaks in the XRD pattern (Figure S2) can be well indexed to Li_2S , implying the formation of Li_2S - LiI solid solution. The particle size of the composite is 0.5-5 μm from the SEM image (Figure S3). The elemental mappings of S, P and I (Figure S4) indicates that the active material and solid electrolyte are uniformly distributed in the cathode composite. The content of Li_2S in the cathode composite is 43.4 wt. %, which is the highest among all the reported Li_2S -based cathodes in all-solid-state batteries.²⁷⁻³² The obtained cathode powders were mixed with polytetrafluoroethylene (PTFE) binder, ground in a mortar, and then rolled into thin sheets. The as-prepared cathode film is then cold-pressed onto a stainless-steel (SS) mesh current collector. The thin-electrolyte layer was prepared by dropping LPS suspension in toluene into a Kevlar nonwoven scaffold, followed by drying overnight under vacuum. Toluene was used as the solvent to prepare the suspension because of its stability with LPS electrolyte,²⁰ as no other peaks can be detected in the XRD of the soaked LPS and all the Raman peaks of the soaked LPS

electrolyte are well matched with pristine LPS powders (Figure S5). Figure S6 shows the SEM images of the LPS-Kevlar membrane after cold pressing, indicating that the membrane is very compact. The ionic conductivity of the LPS-Kevlar membrane is 0.30 mS cm^{-1} (Figure S7), which is slightly lower than that of the pristine LPS pellet (0.56 mS cm^{-1}) because the Kevlar nonwoven scaffold is an ionic insulator. The LPS-Kevlar electrolyte was cold pressed on the cathode film and then a thin Li metal was attached to the top side of the solid electrolyte to make an all-solid-state full cell. The stable voltage profiles of the Li/LPS-Kevlar/Li cell at 0.2 mA cm^{-2} (Figure S8) implies a good interfacial stability between LPS-Kevlar electrolyte and Li. It should be noted that LPS is not thermodynamically stable with Li^{33} and therefore the interfacial stability should be achieved by the formation of passivation interphase. The schematic of such an all-solid-state cell is shown in Figure 2.

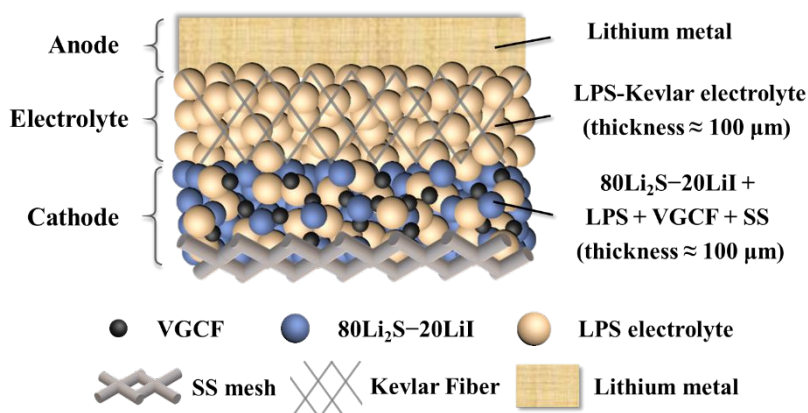


Figure 2. Schematic of the cathode-supported all-solid-state Li–Li₂S cell.

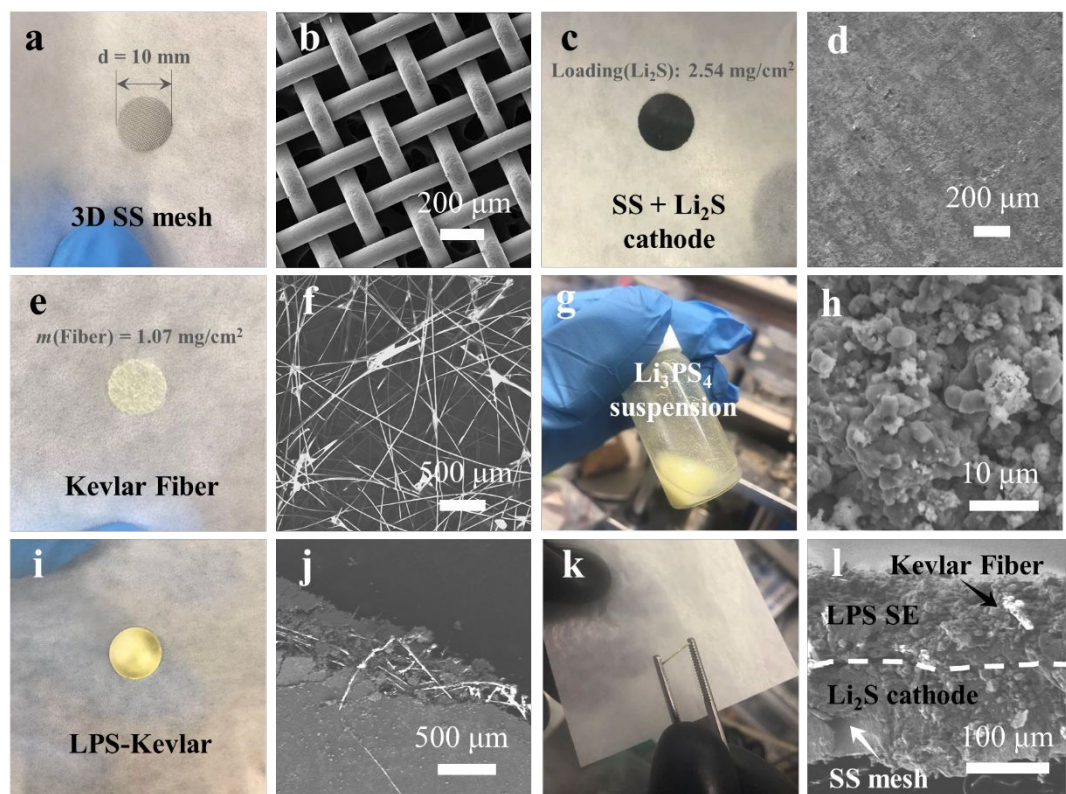


Figure 3. Photos and SEM images of (a,b) SS mesh, (c,d) SS-Li₂S composite cathode, (e,f) Kevlar nonwoven scaffold, (g) Li₃PS₄ electrolyte suspension, (h) Li₃PS₄ dried from the suspension (i,j) Li₃PS₄-Kevlar electrolyte, (k,l) SS mesh supported cathode and Li₃PS₄-Kevlar electrolyte.

The photo and SEM images of the key steps in the fabrication processes of all-solid-state cells are shown in Figure 3. A stainless-steel (SS) mesh with a pore size of around 200 μm (Fig. 3a and 3b) was used as the current collector to enhance the mechanical strength and the integrity of the Li₂S cathode. The unique mesh structure of the current collector allows a high loading of active material (Li₂S: 2.54–7.64 mg cm^{-2}). The Li₂S-LiI active material is uniformly spread on the SS mesh (Fig. 3c and d). The web structure of the Kevlar nonwoven scaffold is shown in Figure 3e and 3f. LPS suspension was prepared in an argon-filled glove box (Figure 3g) and the

dried LPS particles are homogeneous and regular with the sizes of approximately 2-5 μm (Figure 3h). The LPS suspension was dropped into Kevlar nonwoven scaffold with a designed amount to control the thickness of solid electrolytes. Figure 3i and 3j represents the photo and SEM image of the cold-pressed LPS–Kevlar membrane, which clearly shows the reinforced structure.

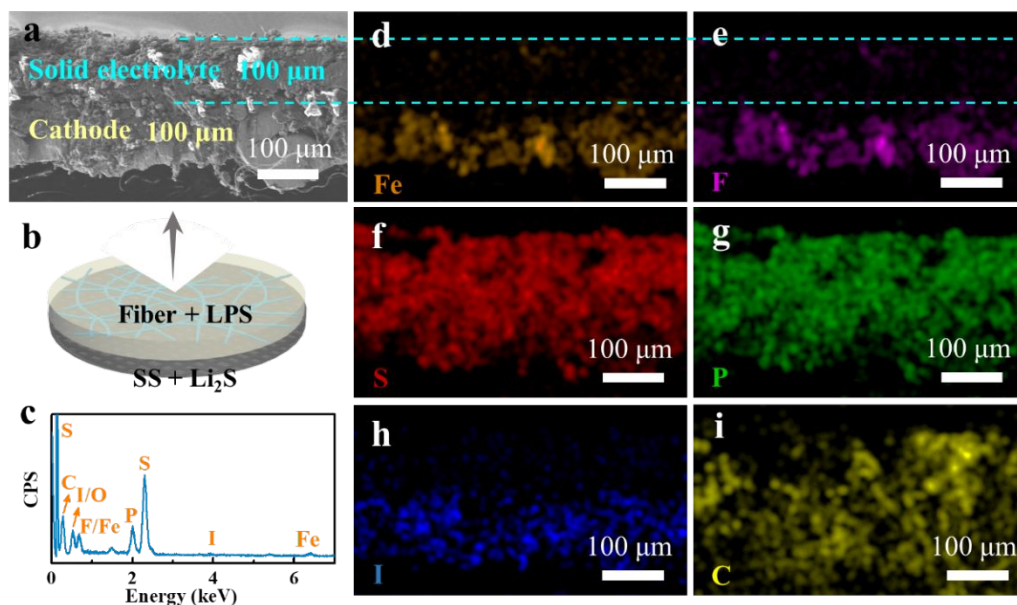


Figure 4. (a) Cross-section SEM image, (b) schematic illustration and (c) EDS of the cathode composite. (d-i) element mappings of Fe, F, S, P, I, and C.

The thicknesses of the electrolyte membrane and the cathode layer were demonstrated from the cross-section SEM images (Figure 3k and 3l and Figure 4a-b). The distribution of the elements from the EDS mappings in Figure 4d-i shows that the thickness of the cathode layer and the electrolyte layer are both about 100 μm , as Fe, F and I are only present in the cathode and P and S are present in both the cathode and the electrolyte. Furthermore, the energy dispersive spectroscopy (EDS) results in Figure 4c confirms the high purity of the sample.

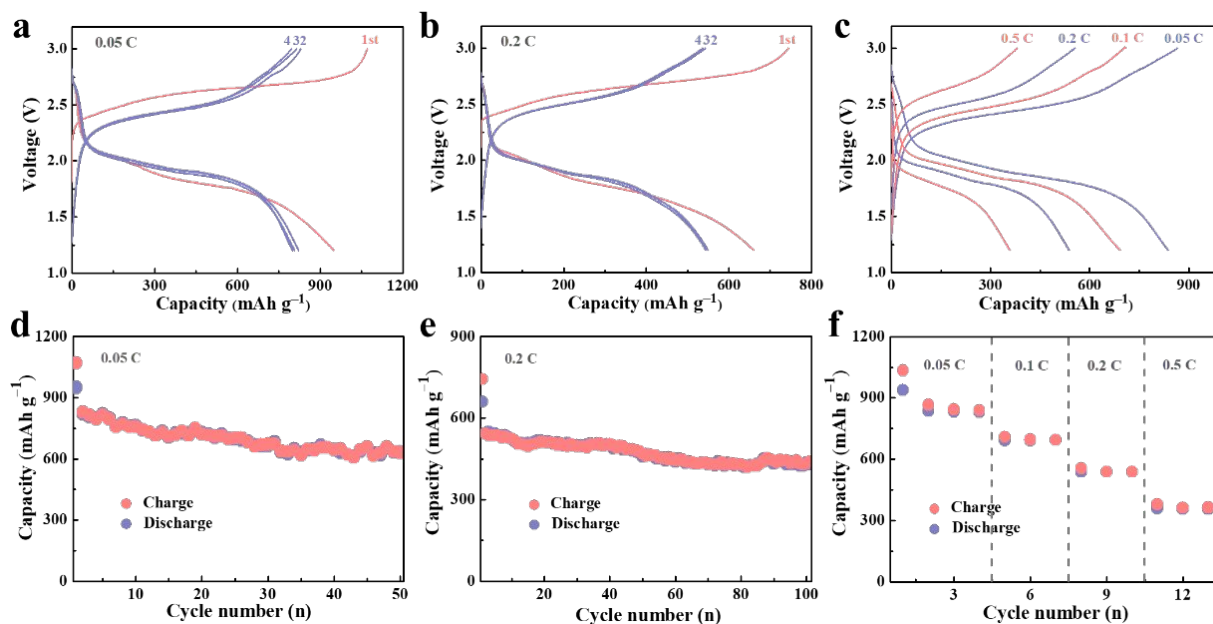


Figure 5. Charge-discharge profiles of the cathode-supported all-solid-state Li-Li₂S cells at (a) 0.05 C, (b) 0.2 C and (c) different rates from 0.05 C to 0.5 C at 25 °C. Cycle performance of the cathode-supported all-solid-state Li-Li₂S cells at (d) 0.05C and (e) 0.2 C at 25 °C. (f) Rate performance of the cathode-supported all-solid-state Li-Li₂S cell at 25 °C. The specific capacities are calculated based on the mass of Li₂S in the cathode composite. The Li₂S loading is 2.54 mg cm⁻².

The electrochemical performances of all-solid-state full cell were evaluated at room temperature.

Figure 5a shows the galvanostatic charge-discharge profiles of the Li-Li₂S solid cell with a Li₂S loading of 2.54 mg cm⁻² in the potential range of 1.2–3.0 V at 0.05 C at room temperature.

Different from the traditional liquid Li/Li₂S cell, only one plateau is observed during charge and discharge processes. No polysulfide intermediates are formed during the conversion reaction that completely solves the issue of shuttle reaction in liquid Li-Li₂S cell.^{25, 30, 34} The cell in the first charge-discharge process displays a charge capacity of 1070.1 mAh g⁻¹ and a high discharge capacity of 949.9 mAh g⁻¹ with a coulombic efficiency of 88.8%. The relatively large

overpotential in the first cycle is attributed to the activation process.²⁵ During the following cycles, the overpotential decreases although it is still relatively large when compared with the cells using LiCoO_2 as the cathode.⁵ Possible reasons for the large overpotential include the addition of PTFE binder in the cathode composite and the low ionic conductivity of the electrolyte. The cell capacity slightly reduced with charge/discharge cycles (Figure 5d). At 50 cycles, the all-solid-state cell with thin electrolyte still shows a high discharge capacity of 636.4 mAh g^{-1} . The excellent capacity retention of the solid cell benefits from the SS mesh current collector. The galvanostatic charge-discharge performance of the cell without SS mesh current collector was also tested (Figure S9a). The cell shows a low initial discharge capacity of 840.5 mAh g^{-1} with a poor cycle performance and large cell resistance (Figure S9b and S10) at 50 cycles. The results show that using SS mesh current collector effectively improve the mechanical integrity of the Li_2S cathode that experienced a huge volume change during charge/discharge process. The cycle performance of the cell at a high rate of 0.2 C is shown in Figure 5b and e. Although the increase of the current rate from 0.05 C to 0.2 C reduces the discharge capacity and enhances the overpotential, the cell still shows high cycling stability at a capacity decay rate of only 1.16 mAh g^{-1} per cycle from cycle 2 to cycle 100. In addition, the active cell exhibits a high rate capability at 25°C (Figure 5c and f). The discharge capacities of 836.9, 692.2, 537.8 and 358.5 mAh g^{-1} are achieved at 0.05, 0.1, 0.2 and 0.5 C, respectively. As one important advantage of all-solid-state batteries is the ability to operate at higher temperatures, we also tested the

electrochemical performance of the cell at 60 °C (Figure S11). The cell was able to cycle stably at 0.1 C and 0.2 C at 60 °C with enhanced kinetics.

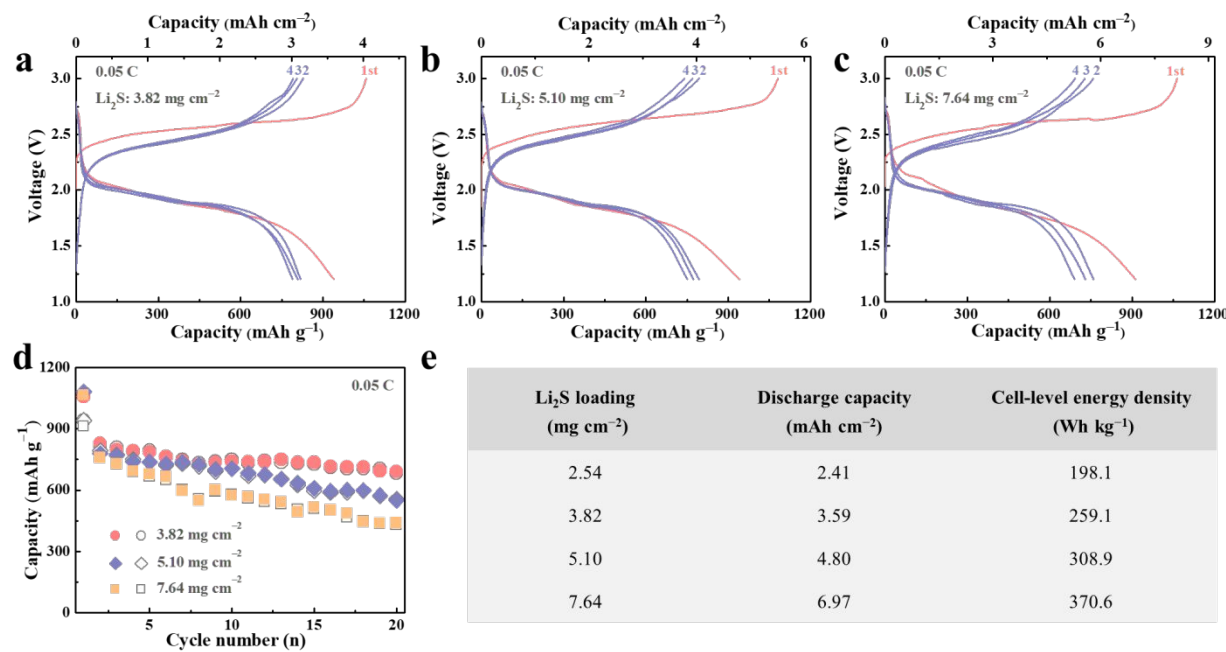


Figure 6. Charge-discharge profiles of the cathode-supported all-solid-state Li-Li₂S cells with a Li₂S loading of (a) 3.82 mg cm⁻², (b) 5.10 mg cm⁻², and (c) 7.64 mg cm⁻² at 0.05 C at 25 °C. (d) Cycle performance of the cathode-supported all-solid-state Li-Li₂S cells with different Li₂S loadings. (e) Cell-level energy densities of the cathode-supported all-solid-state Li-Li₂S cells with different loadings.

We further tested the electrochemical performance of the cells with increased Li₂S loadings. The galvanostatic charge-discharge profiles with the Li₂S loading of 3.82, 5.10 and 7.64 mg cm⁻² are shown in Figure 6a-c. The initial discharge capacities of the three cells with different Li₂S loading are similar, however, the cell with a higher Li₂S loading shows a faster capacity decay (Figure 6d). The cell energy densities with different Li₂S loadings are summarized in Figure 6e.

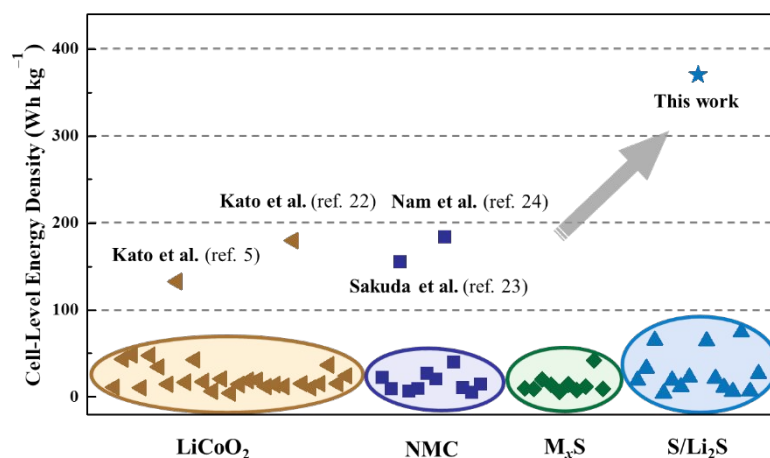


Figure 7. The cell-level energy density of all-solid-state cells using sulfides as the electrolyte. The cells with different cathodes are represented with different colors. More detailed information about the cells can be found in Table S1. Note that the weight of current collectors was not included in the calculation and the cell-level energy density of this work is calculated based on the reversible capacity of the first cycle.

Figure 7 compared the cell energy densities of all the reported sulfide-based all-solid-state cells with the detailed weight of cell component are shown in Table S1. The cell energy density is calculated from the average discharge voltage, cell capacity, and total weights of the cathode, solid electrolyte, and anode, but the weights of the current collectors and exterior package are excluded for calculation due to lack of information from the literature. One reason is that most of the previous reports used a lab-scale Swagelok cell to test the performance of the solid-state battery, wherein two stainless steel (or Ti) rods are used as the current collectors.^{32, 35} As shown in the figure, the cell energy densities of most reported all-solid-state cells with sulfide electrolytes are $< 100 \text{ Wh kg}^{-1}$, which is much lower than that of commercialized liquid cells of $\sim 200 \text{ Wh kg}^{-1}$ due to the utilization of thick solid electrolytes. Our Li/Li₂S solid cell with a high

Li₂S loading of 7.64 mg cm⁻² exceeds energy density of 370 Wh kg⁻¹ in cell level for the first cycle, which is the highest energy density reported to date. It should be noted that the cell-level energy density of the cell is not high if the weight of the SS mesh current collector is included in the calculation. Since the main purpose of using SS mesh as the current collector is to provide a matrix for the cathode composite, other electronically conducting materials with a 2D or 3D structure but with a lower density can also be used as the current collector. For example, the cell-level energy density (including current collectors) of the cell was largely increased (from 59 to 159 Wh kg⁻¹) by replacing SS mesh (53.3 mg cm⁻²) with Ni-coated Kevlar fiber (1.22 mg cm⁻²) as the current collector (Figure S12).

In summary, we demonstrate a thick cathode supported all-solid-state lithium batteries with a thin electrolyte (~100 μm). LPS–Kevlar solid electrolyte membranes are formed by dropping the LPS suspension into the Kevlar nonwoven scaffold followed by drying/cold pressing onto a thick SS mesh supported Li₂S–LiI cathode. Using Li metal anode, the Li/Li₂S cell with 2.54 mg cm⁻¹ Li₂S loading achieves a high reversible discharge capacity of 949.9 mAh g⁻¹ at 0.05 C and stable cycling for 100 cycles at 0.2 C. All-solid-state Li–Li₂S cell with a high Li₂S loading of 7.64 mg cm⁻¹ exhibits an extremely high cell-based energy density of 370.6 Wh kg⁻¹.

ASSOCIATED CONTENT

Supporting Information. The Supporting Information is available free of charge on the ACS publication website at DOI:

Impedance plot of the SS/80Li₂S-20Li/SS cell, XRD pattern and SEM images of the cathode composite, XRD patterns and Raman spectra of the as-prepared LPS and LPS dried from the LPS suspension in toluene, SEM images of the surface of LPS–Kevlar electrolyte, Nyquist plots of blocking cells, Galvanostatic cycling of the Li/LPS–Kevlar/Li cell, Charge-discharge profiles and cycle performance of Li–Li₂S solid cells without SS mesh current collector, Nyquist plots of the Li–Li₂S cells, Charge-discharge profiles of the cathode-supported all-solid-state Li–Li₂S cells at 60 °C, Charge-discharge of the all-solid-state Li–Li₂S cell with Ni coated Kevlar nonwoven as the current collector for the cathode, Summary of the cell-level energy densities of all-solid-state cells using sulfides as the electrolyte (PDF)

AUTHOR INFORMATION

Corresponding Author

*Email: fdhan@umd.edu

*Email: piliu@eng.ucsd.edu

*Email: cswang@umd.edu

Notes

The authors declare no competing financial interest.

ACKNOWLEDGMENT

This work is supported by the U.S. Department of Energy ARPA-E (Award No. DE-AR0000781).

REFERENCES

- (1) Hu, Y.-S. Batteries: Getting Solid. *Nature Energy* **2016**, *1* (4), 16042.
- (2) Janek, J.; Zeier, W. G. A Solid Future for Battery Development. *Nature Energy* **2016**, *1* (9), 16141.
- (3) Li, J. C.; Ma, C.; Chi, M. F.; Liang, C. D.; Dudney, N. J. Solid Electrolyte: the Key for High-Voltage Lithium Batteries. *Adv. Energy Mater.* **2015**, *5* (4), 1401408.
- (4) Kamaya, N.; Homma, K.; Yamakawa, Y.; Hirayama, M.; Kanno, R.; Yonemura, M.; Kamiyama, T.; Kato, Y.; Hama, S.; Kawamoto, K.; et al. Lithium Superionic Conductor. *Nat. Mater.* **2011**, *10* (9), 682-686.
- (5) Kato, Y.; Hori, S.; Saito, T.; Suzuki, K.; Hirayama, M.; Mitsui, A.; Yonemura, M.; Iba, H.; Kanno, R. High-Power All-Solid-State Batteries Using Sulfide Superionic Conductors. *Nat. Energy* **2016**, *1* (4), 16030.
- (6) Seino, Y.; Ota, T.; Takada, K.; Hayashi, A.; Tatsumisago, M. A Sulphide Lithium Super Ion Conductor is Superior to Liquid Ion Conductors for Use in Rechargeable Batteries. *Energy Environ. Sci.* **2014**, *7* (2), 627-631.
- (7) Mizuno, F.; Hayashi, A.; Tadanaga, K.; Tatsumisago, M. New, Highly Ion-Conductive Crystals Precipitated from Li_2S - P_2S_5 Glasses. *Adv. Mater.* **2005**, *17* (7), 918-921.

- (8) Kanno, R.; Murayama, M. Lithium Ionic Conductor Thio-LISICON: The $\text{Li}_2\text{S-GeS}_2\text{-P}_2\text{S}_5$ System. *Journal of The Electrochemical Society* **2001**, *148* (7), A742-A746.
- (9) Zhou, L.; Park, K.-H.; Sun, X.; Lalère, F.; Adermann, T.; Hartmann, P.; Nazar, L. F. Solvent-Engineered Design of Argyrodite $\text{Li}_6\text{PS}_5\text{X}$ (X = Cl, Br, I) Solid Electrolytes with High Ionic Conductivity. *ACS Energy Letters* **2018**, *4* (1), 265-270.
- (10) Yao, X. Y.; Huang, N.; Han, F. D.; Zhang, Q.; Wan, H. L.; Mwizerwa, J. P.; Wang, C. S.; Xu, X. X. High-Performance All-Solid-State Lithium-Sulfur Batteries Enabled by Amorphous Sulfur-Coated Reduced Graphene Oxide Cathodes. *Adv. Energy Mater.* **2017**, *7* (17), 1602923.
- (11) Han, F.; Yue, J.; Fan, X.; Gao, T.; Luo, C.; Ma, Z.; Suo, L.; Wang, C. High-Performance All-Solid-State Lithium-Sulfur Battery Enabled by a Mixed-Conductive Li_2S Nanocomposite. *Nano Lett.* **2016**, *16* (7), 4521-4527.
- (12) Nagata, H.; Chikusa, Y. A Lithium Sulfur Battery with High Power Density. *J. Power Sources* **2014**, *264*, 206-210.
- (13) Moon, C. K.; Lee, H.-J.; Park, K. H.; Kwak, H.; Heo, J. W.; Choi, K.; Yang, H.; Kim, M.-S.; Hong, S.-T.; Lee, J. H.; et al. Vacancy-Driven Na^+ Superionic Conduction in New Ca-Doped Na_3PS_4 for All-Solid-State Na-Ion Batteries. *ACS Energy Letters* **2018**, *3* (10), 2504-2512.
- (14) Suzuki, K.; Kato, D.; Hara, K.; Yano, T.-A.; Hirayama, M.; Hara, M.; Kanno, R. Composite Sulfur Electrode Prepared by High-Temperature Mechanical Milling for use in an All-Solid-State Lithium-Sulfur Battery with a $\text{Li}_{3.25}\text{Ge}_{0.25}\text{P}_{0.75}\text{S}_4$ Electrolyte. *Electrochim. Acta* **2017**, *258*, 110-115.

- (15) Busche, M. R.; Weber, D. A.; Schneider, Y.; Dietrich, C.; Wenzel, S.; Leichtweiss, T.; Schröder, D.; Zhang, W.; Weigand, H.; Walter, D.; et al. In Situ Monitoring of Fast Li-Ion Conductor $\text{Li}_7\text{P}_3\text{S}_{11}$ Crystallization Inside a Hot-Press Setup. *Chem. Mater.* **2016**, 28 (17), 6152-6165.
- (16) Lin, Z.; Liu, Z.; Fu, W.; Dudney, N. J.; Liang, C. Lithium Polysulfidophosphates: A Family of Lithium-Conducting Sulfur-Rich Compounds for Lithium-Sulfur batteries. *Angew. Chem. Int. Ed. Engl.* **2013**, 52 (29), 7460-7463.
- (17) Nagata, H.; Chikusa, Y. All-Solid-State Lithium-Sulfur Battery with High Energy and Power Densities at the Cell Level. *Energy Technol.* **2016**, 4 (4), 484-489.
- (18) Lin, Z.; Liu, Z.; Dudney, N. J.; Liang, C. Lithium Superionic Sulfide Cathode for All-Solid Lithium-Sulfur Batteries. *Acs Nano* **2013**, 7 (3), 2829-2833.
- (19) Whiteley, J. M.; Taynton, P.; Zhang, W.; Lee, S. H. Ultra-thin Solid-State Li-Ion Electrolyte Membrane Facilitated by a Self-Healing Polymer Matrix. *Adv. Mater.* **2015**, 27 (43), 6922-6927.
- (20) Nam, Y. J.; Cho, S. J.; Oh, D. Y.; Lim, J. M.; Kim, S. Y.; Song, J. H.; Lee, Y. G.; Lee, S. Y.; Jung, Y. S. Bendable and Thin Sulfide Solid Electrolyte Film: A New Electrolyte Opportunity for Free-Standing and Stackable High-Energy All-Solid-State Lithium-Ion Batteries. *Nano Lett.* **2015**, 15 (5), 3317-3323.
- (21) Hood, Z. D.; Wang, H.; Pandian, A. S.; Peng, R.; Gilroy, K. D.; Chi, M.; Liang, C.; Xia, Y. Fabrication of Sub-Micrometer-Thick Solid Electrolyte Membranes of $\beta\text{-Li}_3\text{PS}_4$ via Tiled Assembly of Nanoscale, Plate-Like Building Blocks. *Adv. Energy Mater.* **2018**, 8 (21), 1800014.

- (22) Kato, Y.; Shiotani, S.; Morita, K.; Suzuki, K.; Hirayama, M.; Kanno, R. All-Solid-State Batteries with Thick Electrode Configurations. *J. Phys. Chem. Lett.* **2018**, *9* (3), 607-613.
- (23) Sakuda, A.; Kuratani, K.; Yamamoto, M.; Takahashi, M.; Takeuchi, T.; Kobayashi, H. All-Solid-State Battery Electrode Sheets Prepared by a Slurry Coating Process. *J. Electrochem. Soc.* **2017**, *164* (12), A2474-A2478.
- (24) Nam, Y. J.; Oh, D. Y.; Jung, S. H.; Jung, Y. S. Toward Practical All-Solid-State Lithium-Ion Batteries with High Energy Density and Safety: Comparative Study for Electrodes Fabricated by Dry- and Slurry-Mixing Processes. *J. Power Sources* **2018**, *375*, 93-101.
- (25) Hakari, T.; Hayashi, A.; Tatsumisago, M. Li₂S-Based Solid Solutions as Positive Electrodes with Full Utilization and Superlong Cycle Life in All-Solid-State Li/S Batteries. *Adv. Sustainable Syst.* **2017**, *1* (6), 1700017.
- (26) Hakari, T.; Hayashi, A.; Tatsumisago, M. Highly Utilized Lithium Sulfide Active Material By Enhancing Conductivity In All-Solid-State Batteries. *Chem. Lett.* **2015**, *44* (12), 1664-1666.
- (27) Takeuchi, T.; Kageyama, H.; Nakanishi, K.; Ohta, T.; Sakuda, A.; Sakaebe, H.; Kobayashi, H.; Tatsumi, K.; Ogumi, Z. Rapid Preparation of Li₂S-P₂S₅ Solid Electrolyte and Its Application for Graphite/Li₂S All-Solid-State Lithium Secondary Battery. *ECS Electrochem. Lett.* **2014**, *3* (5), A31-A35.
- (28) Nagao, M.; Hayashi, A.; Tatsumisago, M. Sulfur–Carbon Composite Electrode for All-Solid-State Li/S Battery with Li₂S–P₂S₅ Solid Electrolyte. *Electrochim. Acta* **2011**, *56* (17), 6055-6059.

- (29) Yang, Y.; Zheng, G.; Misra, S.; Nelson, J.; Toney, M. F.; Cui, Y. High-Capacity Micrometer-Sized Li_2S Particles as Cathode Materials for Advanced Rechargeable Lithium-Ion Batteries. *J Am Chem Soc* **2012**, *134* (37), 15387-15394.
- (30) Nagao, M.; Hayashi, A.; Tatsumisago, M. High-Capacity Li_2S -Nanocarbon Composite Electrode for All-Solid-State Rechargeable Lithium Batteries. *J. Mater. Chem. A* **2012**, *22* (19), 10015-10020.
- (31) Hayashi, A.; Ohtsubo, R.; Ohtomo, T.; Mizuno, F.; Tatsumisago, M. All-Solid-State Rechargeable Lithium Batteries with Li_2S as a Positive Electrode Material. *J. Power Sources* **2008**, *183* (1), 422-426.
- (32) Nagao, M.; Hayashi, A.; Tatsumisago, M.; Ichinose, T.; Ozaki, T.; Togawa, Y.; Mori, S. Li_2S Nanocomposites Underlying High-Capacity and Cycling Stability in All-Solid-State Lithium-Sulfur Batteries. *J. Power Sources* **2015**, *274*, 471-476.
- (33) Han, F. D.; Zhu, Y. Z.; He, X. F.; Mo, Y. F.; Wang, C. S., Electrochemical Stability of $\text{Li}_{10}\text{GeP}_2\text{S}_{12}$ and $\text{Li}_7\text{La}_3\text{Zr}_2\text{O}_{12}$ Solid Electrolytes. *Adv. Energy Mater.* **2016**, *6* (8), 1501590.
- (34) Mikhaylik, Y. V.; Akridge, J. R. Polysulfide Shuttle Study in the Li/S Battery System. *Journal of The Electrochemical Society* **2004**, *151* (11), A1969-A1976.
- (35) Aso, K.; Sakuda, A.; Hayashi, A.; Tatsumisago, M., All-Solid-State Lithium Secondary Batteries Using NiS -Carbon Fiber Composite Electrodes Coated With Li_2S - P_2S_5 Solid Electrolytes By Pulsed Laser Deposition. *ACS Appl. Mater. Interfaces* **2013**, *5* (3), 686-690.